

Letter to the Editor

## Energy spectrum of secondary protons above the atmosphere measured by the instruments NINA and NINA-2

V. Bidoli<sup>1</sup>, M. Casolino<sup>1</sup>, M. De Pascale<sup>1</sup>, G. Furano<sup>1</sup>, A. Iannucci<sup>1</sup>, A. Morselli<sup>1</sup>, P. Picozza<sup>1</sup>, R. Sparvoli<sup>1</sup>, A. Bakaldin<sup>2</sup>, A. Galper<sup>2</sup>, S. Koldashov<sup>2</sup>, M. Korotkov<sup>2</sup>, A. Leonov<sup>2</sup>, V. Mikhailov<sup>2</sup>, S. Voronov<sup>2</sup>, M. Boezio<sup>3</sup>, V. Bonvicini<sup>3</sup>, A. Vacchi<sup>3</sup>, G. Zampa<sup>3</sup>, N. Zampa<sup>3</sup>, M. Ambriola<sup>4</sup>, F. Cafagna<sup>4</sup>, M. Circella<sup>4</sup>, C. De Marzo<sup>4</sup>, O. Adriani<sup>5</sup>, P. Papini<sup>5</sup>, P. Spillantini<sup>5</sup>, S. Straulino<sup>5</sup>, E. Vannuccini<sup>5</sup>, M. Ricci<sup>6</sup>, and G. Castellini<sup>7</sup>

<sup>1</sup>University of Rome “Tor Vergata” and INFN section of Roma2, Rome, Italy

<sup>2</sup>Moscow Engineering Physics Institute, Moscow, Russia

<sup>3</sup>University of Trieste and INFN section of Trieste, Trieste, Italy

<sup>4</sup>University of Bari and INFN section of Bari, Bari, Italy

<sup>5</sup>University of Florence and INFN section of Florence, Florence, Italy

<sup>6</sup>INFN National Laboratories of Frascati, Frascati, Italy

<sup>7</sup>Institute of Applied Physics “Nello Carrara”, CNR, Florence, Italy

Received: 28 March 2002 – Revised: 21 May 2002 – Accepted: 28 May 2002

**Abstract.** In this paper we report on the energy spectrum of protons of albedo origin measured by the instruments NINA and NINA-2 at different geomagnetic locations, and the behaviour of the proton flux as a function of altitude out of the South Atlantic Anomaly. The instrument NINA was used on board the satellite Resurs-01-N4 between 1998 and 1999, at an altitude of about 830 km. The NINA-2 apparatus, on board the satellite MITA, was put into orbit in July 2000, at an altitude of about 450 km. A detailed understanding of the fluxes of charged particles in near Earth orbit is important to reach an accurate theoretical description of the Earth’s magnetic field, but also as input for the calculation of the background for scientific instruments aboard satellites, like the future AGILE and GLAST  $\gamma$  astronomy telescopes.

**Key words.** Magnetospheric physics (energetic particles, trapped; instruments and techniques)

### 1 Introduction

The NINA mission, the first step in a Russian-Italian scientific program, was aimed at studying the nuclear component of cosmic rays from hydrogen to iron across the energy range 10–200 MeV/n in the vicinity of the Earth, by using space-borne instruments. This first mission, which started on 10 July 1998, was carried out aboard the Russian satellite Resurs-01-N4, and provided measurements of Galactic Cosmic Ray (GCR) fluxes (Bidoli et al., 2001), the isotopic composition of Solar Energetic Particles (SEP) (Bakaldin et al.,

2001) and the composition of particles trapped in the Radiation Belts (Bakaldin et al., 2002).

NINA stopped being operational in mid 1999. On 15 July 2000, a second detector, NINA-2, was put into orbit in the Italian satellite MITA, in order to continue the scientific program of the NINA instrument in extending its measurements in a different phase of the solar cycle.

This paper is focused on the measurements of the proton energy spectrum below the geomagnetic cutoff, taken by NINA and NINA-2, in regions of equatorial latitude. It is well known that the interaction of cosmic rays with residual atmosphere produces secondary particles. The secondary particle flux is composed mainly of electrons, positrons, protons, neutrons and gamma-rays, but also light nuclei. Some fraction of secondary charged particles, with rigidity less than the local geomagnetic cutoff, can travel backward along the magnetic field line connected to the point of observation. Depending on their pitch angle, such particles can only make one bounce (and are called *albedo* particles) or more than one bounce (*quasi-trapped* particles) in the geomagnetic field. There is also a fraction of secondary particles that can remain *trapped* for several years.

Measurements of the energy spectra of secondary protons were carried out on board the Space Shuttle by the AMS instrument (Alcaraz et al., 2000), which went into space in June 1998. Subsequent theoretical speculations, which investigated the behaviour of primary and secondary particles in the geomagnetic field, confirmed the secondary origin of the particles measured by AMS (Derome et al., 2000; Lipari, 2002). The measurements of AMS cover the energy interval from 0.1 to 200 GeV. Below 100 MeV, no recent accurate measurements of albedo protons above the atmosphere are available.

Correspondence to: R. Sparvoli  
(Roberta.Sparvoli@roma2.infn.it)

The study of secondary fluxes is an important test of the quality of our current description of geomagnetic effects, including an accurate description of the Earth's magnetic field and of the particle propagation in it. A detailed understanding of the fluxes of charged particles at low altitude is even more important since it serves as input for the calculation of the background for future satellite instruments, such as the planned AGILE and GLAST  $\gamma$  astronomy telescopes (Lipari, 2002). These instruments plan to be operative in the energy region starting from  $\sim 30$  MeV up to 50 GeV (AGILE) and several hundred GeV (GLAST). They will both fly on equatorial orbits, at an altitude of about 500 km. For such orbits, the charged particle background is composed of electrons, positrons, primary and secondary protons.

NINA and NINA-2 performed extensive measurements of the proton flux between 10 and 35 MeV. With this new data the knowledge of the secondary proton flux at low energies will be precise, leading to accurate estimations of background for gammas.

## 2 The NINA experiments

The satellite Resurs-01-N4 had a near-Earth polar orbit with a  $98^\circ$  inclination and 835 km altitude. The instrument NINA is housed in Resurs on the top side external to the satellite, so as to point always to the zenith. The period of observation taken under consideration ranges from November 1998 to April 1999; after this date, problems with the onboard transmitter stopped the data download (Bidoli et al., 2001).

The satellite MITA, housing the instrument NINA-2, was put into an almost circular polar orbit, with an inclination of about  $87.3^\circ$  and an altitude of about 450 km. Data recording started in July 2000. The last data was taken in August 2001, at an altitude of approximately 240 km, when the last radio contact was possible. The satellite had a three-axis stabilization, and measurements were carried out in two different modes: zenith orientation (axis of the instrument towards the zenith) and Sun orientation (axis of the instrument pointing to the Sun; Casolino et al., 1999, 2001).

### 2.1 The silicon detector

The NINA and NINA-2 instruments were based on the identical silicon *detector*, composed of 16  $X - Y$  planes, each consisting of two  $n$ -type silicon elements,  $60 \times 60 \text{ mm}^2$ , divided into 16 strips. The plane thickness is  $(2 \times 150) \mu\text{m}$  for the first plane, and  $(2 \times 380) \mu\text{m}$  for the remaining 15 planes: the active part thus amounts to 11.7 mm. Interplanar distance is 1.4 cm for planes between 2 and 16, and 8.5 cm between plane 1 and 2, in order to improve the determination of the particle incident angle. The angular aperture of the telescope is about  $32^\circ$ .

The whole structure is surrounded by a cylindrical aluminium vessel 2 mm thick, aside from a  $300 \mu\text{m}$  thick window placed in front of the detector. The instrument has two different modes of particle detection: Low Threshold and

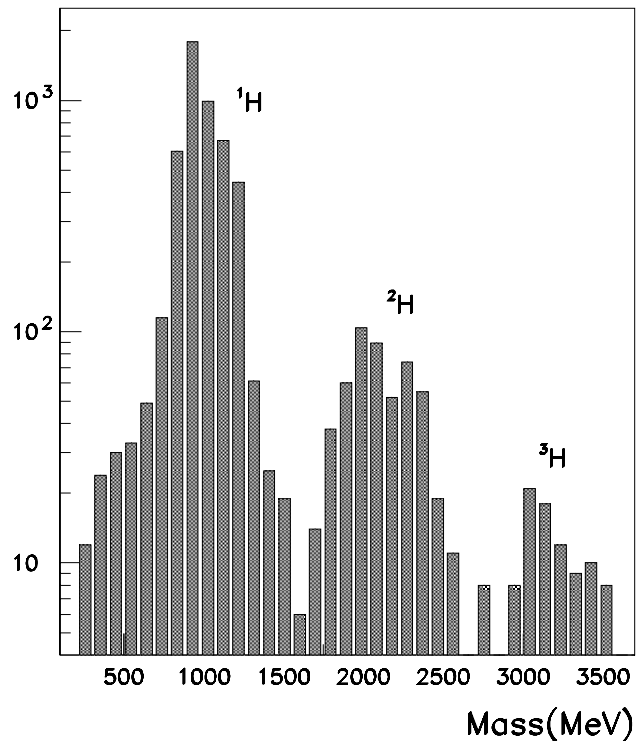


**Fig. 1.** Mass distribution of particles with charge  $Z = 1$  at L-shell  $< 3$  and  $B > 0.26$  G, as measured by NINA-2.

High Threshold. In the first configuration, the telescope can detect nuclei from hydrogen to iron across the full energy range (10–200 MeV/n), whereas in High Threshold mode it is possible to detect hydrogen isotopes only across a narrow energy range (11–16 MeV).

The instrument performance was estimated by means of Monte Carlo simulations based on the CERN-GEANT code (Brun et al., 1994). In addition, both detectors were calibrated at accelerator laboratories, with beam species from hydrogen to oxygen, in a wide energy interval. The geometric factor of the instrument ranges from  $8.6 \text{ cm}^2 \text{ sr}$  for low energy particles to  $1 \text{ cm}^2 \text{ sr}$  for particles crossing the whole detector. The mass resolution of the instrument is about 0.15 amu for He isotopes and about 0.1 amu for H isotopes. The energy resolution is better than 1 MeV. A detailed description of the instrument and its performance with beam facilities and in orbit are reported in the works by Bakaldin et al. (1997); Bidoli et al. (1999, 2001).

### 2.2 Data analysis

The optimal performance of NINA and NINA-2 detectors in terms of charge, mass and energy determination is achieved by requiring the full containment of the particle inside the detector (up to  $\sim 50$  MeV for protons). In addition, a dedicated off-line track selection algorithm is applied, which rejects upward moving particles, tracks accompanied by nuclear interactions, and events consisting of two or more tracks. In order to calculate the energy deposit of the crossing particles

in each layer of the detector, their incident angles are taken into account. A detailed description of the selection algorithm can be found in Bidoli et al. (2001).

Charge and mass identification procedures are applied to events which survive the track selection algorithm. The mass  $M$  and the charge  $Z$  of the particles are calculated in parallel by two methods, in order to have more precise particle recognition: one method uses the residual range (Cook et al., 1993; Hasebe et al., 1993), while the other uses an approximation of the Bethe-Bloch theoretical curve (Bidoli et al., 2001).

For a complete rejection of the background, only particles with the same final identification given by the two methods are selected. Finally, a consistency test for the event is performed by cross-checking the real range of the particle in the detector with the expected value according to simulation.

The particle identification algorithm was tested previously with beam test data and in the Galactic Cosmic Rays (GCR) analysis. It was found that these cuts also eliminate, together with the background, about 3% of tracks of real good particles. Data were corrected for this factor.

As a first step to determine the energy of the detected particles, the sum of the energy deposits in the whole detector is calculated; energy losses in the dead layers between the silicon planes (see Bidoli et al., 2001) are then determined by interpolation formulas. Finally, the incoming energy of the particles in front of the aluminium window is reconstructed by an iterative algorithm, based on the Bethe-Bloch formula using the known particle incident angle.

To evaluate the position of the satellite we use data from NORAD<sup>1</sup>, while the geomagnetic coordinates L-shell and  $B$  are calculated by means of the IGRF<sup>2</sup> model.

To reconstruct the fluxes of a selected isotope, particles for which the estimated value of mass is at more than two standard deviations from the isotope mass are rejected, and compensation for good events lost in the tails of the distribution is given. The differential energy spectrum for particles detected inside a specified region of known geomagnetic coordinates is finally determined by the following formula:

$$Flux(E) = \frac{\Delta N(E)}{T G(E) \Delta E}, \quad (1)$$

where  $\Delta N(E)$  is the number of detected particles in the energy interval  $E \pm \Delta E/2$ ,  $T$  is the exposure time in orbit for the period under consideration,  $G(E)$  is the average value of the geometrical factor in the same interval  $E \pm \Delta E/2$ , and  $\Delta E$  is the energy bin chosen to plot the flux.

### 3 Results and discussion

Along its polar orbit, NINA can measure particles of galactic origin, albedo particles coming from secondary production, as well as particles trapped in the radiation belts. To separate the different families of particles, selections based on L-shell

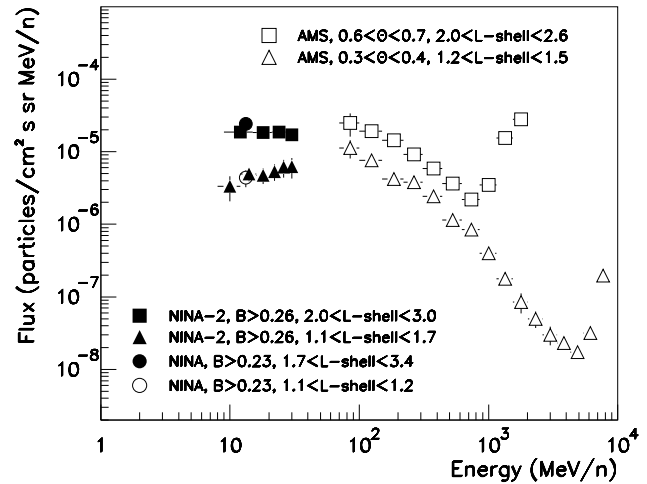


Fig. 2. Differential energy spectra of secondary protons, as measured by NINA and NINA-2, at different L-shell ranges. For comparison, data from the AMS experiment are also presented.

and  $B$  are used; in particular, our analysis has shown that pure albedo and geomagnetically trapped components without contamination from galactic and solar particles, even during intense SEP events, are selected by  $L\text{-shell} < 3$  in NINA's energy range. At  $L\text{-shell} < 3$ , in fact, the geomagnetic cutoff is much higher than the particles' rigidity in NINA's energy interval, so galactic protons of energy  $E < 100$  MeV/n cannot reach neither Resurs nor MITA orbits. It is known, finally, that the geomagnetic cutoff can vary in case of intense SEP events, but during NINA and NINA-2 mission lifetimes, none of these events changed appreciably the particle count rate at  $L\text{-shell} < 3$ .

Figure 1 presents the mass reconstruction for particles with unitary charge, detected by NINA-2 in the restricted region  $L\text{-shell} < 3$  and  $B > 0.26$  G (a region in which both the trapped and the galactic component are eliminated). The mass resolution obtained in orbit is slightly worse than in beam tests, because electronic calibration during the flight, done automatically, can occasionally take place in the south Atlantic anomaly, where the intense count rate affects the measurements. From Fig. 1 it is evident that NINA-2 detected the three hydrogen isotopes.

Secondary nuclei of deuterium above the atmosphere were also observed by the AMS experiment (Lamanna et al., 2001) at energy greater than 150 MeV/n. As is visible in Fig. 1, in NINA's energy range, deuterium and tritium constitute a non-negligible component, so a mass discrimination at least as good as that of both NINA and NINA-2 is needed in order to select a pure sample of protons.

Secondary background produced by cosmic rays inside the instrument must be considered as well. Estimations of this background by means of the method described in Bakaldin et al. (2002), which considers the first silicon detector as a target for secondary production, show that the contribution of this background to the proton count rate is less than 5%.

Figure 2 presents the proton flux, averaged in longitude,

<sup>1</sup> <http://oig1.gsfc.nasa.gov/scripts/foxweb.exe/app01>

<sup>2</sup> <http://nssdc.gsfc.nasa.gov/space/model/magnetos/igrf.html>

**Table 1.** Table of proton fluxes (in particles/cm<sup>2</sup> s sr MeV/n) measured by NINA-2 as a function of energy (rows, in MeV) in different L-shell intervals (columns)

	1.0 < L < 1.1	1.0 < L < 1.7	1.0 < L < 2.6
10	$(4.8 \pm 2.1) \times 10^{-6}$	$(3.3 \pm 1.3) \times 10^{-6}$	$(16.0 \pm 3.7) \times 10^{-6}$
14	$(3.9 \pm 1.3) \times 10^{-6}$	$(5.0 \pm 1.0) \times 10^{-6}$	$(13.0 \pm 2.2) \times 10^{-6}$
18	$(3.4 \pm 1.4) \times 10^{-6}$	$(4.7 \pm 1.5) \times 10^{-6}$	$(12.0 \pm 2.5) \times 10^{-6}$
22	$(2.1 \pm 1.2) \times 10^{-6}$	$(5.3 \pm 1.4) \times 10^{-6}$	$(14.0 \pm 3.0) \times 10^{-6}$
26	$(3.8 \pm 1.9) \times 10^{-6}$	$(6.1 \pm 1.7) \times 10^{-6}$	$(12.0 \pm 3.2) \times 10^{-6}$
30	–	$(6.3 \pm 2.0) \times 10^{-6}$	$(9.9 \pm 3.3) \times 10^{-6}$

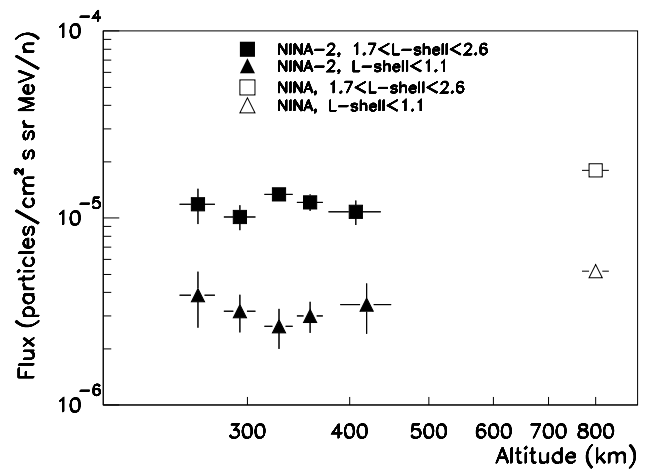
reconstructed in sub-cutoff regions by NINA and NINA-2 at different geomagnetic latitudes. NINA default operating mode was High Threshold, while NINA-2, thanks to its improved onboard computer capabilities, could operate in Low Threshold mode, thus extending the sensitive energy window for protons. The NINA-2 results include data collected in both zenith and Sun orientation, as no statistically significant difference between the two orientations was found. In addition, no distinction was made between albedo and quasi-trapped particles.

Figure 2 shows that the results from NINA and NINA-2 at  $\sim 13$  MeV are in good agreement. The two experiments flew in different periods of the 23rd solar cycle. The agreement confirms that the albedo component comes from the interaction of high energy cosmic rays – above the geomagnetic cutoff – with the atmosphere, and so it is only marginally affected by solar modulation. In the same picture, AMS results at higher energy ( $E > 100$  MeV) are presented as well (Alcaraz et al., 2000).

Table 1 reports on the NINA-2 proton fluxes, averaged in longitude, as a function of energy (rows, in MeV) for six different energies, in three different L-shell intervals (columns). The behaviour of fluxes with longitude was also investigated and some variations were found. The level of such a variation is a factor of 2, with the minimum value reached at the east boundary of the south Atlantic anomaly.

The low-energy data added by NINA and NINA-2 show that the energy spectrum of secondary protons at low energy cannot be simply extrapolated by a power law from AMS data. Indeed, below 100 MeV the spectrum flattens. This feature of the spectrum, already partially foreseen by calculations (Derome et al., 2000), should be taken into account in the construction of background models for gamma-ray telescopes.

In the last months of NINA-2's lifetime, the altitude was decreasing constantly. From an initial altitude of about 450 km, in July 2001, it decreased to about 200 km, and this allowed for the monitoring of albedo proton flux at different altitudes. Figure 3 shows the proton flux versus altitude measured by NINA and NINA-2 across the energy range 12–16 MeV, in two different L-shell intervals and for



**Fig. 3.** Secondary proton flux as a function of altitude, as measured by NINA and NINA-2. Open points: data taken by NINA at  $B > 0.23$  G. Solid points: data taken by NINA-2 at  $B > 0.26$  G. Squares: data for  $1.7 < L\text{-shell} < 2.6$ . Triangles: data for  $L\text{-shell} < 1.1$ .

$B > 0.26$  G, corresponding to albedo fluxes; the solid points represent the measurement taken by NINA-2 at different altitudes, while the open points come from NINA at the altitude of about 830 km. From this picture it is possible to infer that the proton flux at  $\sim 10$  MeV does not depend appreciably on the altitude along a fixed L-shell, in the range from 200 km to 850 km. In the work by Alcaraz et al. (2000), it was shown that quasi-trapped protons detected by AMS at fixed altitude originated from a restricted geographic region. It is plausible to think that the structure of this region depends on the acceptance angle of the detector and its orientation, as well as on the altitude. Small variations in fluxes measured by NINA and NINA-2 at different altitudes, such as those visible in Fig. 3, could therefore be attributed to this.

#### 4 Conclusions

Energy spectra of secondary sub-cutoff protons were measured at different geomagnetic latitudes across the energy

range 10–35 MeV by the space instruments NINA and NINA-2. The good instrument capabilities allowed for measurements of the spectra of protons with high accuracy, also taking into account the contribution of deuterium and tritium, which amounted to about 10%. The proton energy spectra were found to be practically flat in this energy range and not to vary appreciably with altitude. In addition, the measured flux was approximately constant between 1998 and 2001.

*Acknowledgements.* The Editor in chief thanks I. Dandouras for his help in evaluating this paper.

## References

- Alcaraz, J., Alvisi, D., Alpat, B., et al.: Protons in near Earth orbit, *Physics Letter B*, 472, 215–226, 2000.
- Bakaldin, A., Barbiellini, G., Bertolucci, S., et al.: Experiment NINA: investigation of low energy nuclear fluxes in the near-Earth space, *Astroparticle Physics*, 8, 109–130, 1997.
- Bakaldin, A., Galper, A., Koldashov, S., et al.: Light Isotope Abundances in Solar Energetic Particles measured by the Space Instrument NINA, astro-ph/0106390, 2001.
- Bakaldin, A., Galper, A., Koldashov, S., et al.: Geomagnetically trapped light isotopes observed with the detector NINA, *Journal of Geophysical Research, Space Physics*, in press, 2002.
- Bidoli, V., Casolino, M., de Pascale, M. P., et al.: The space telescope NINA: results of a beam test calibration, *NIM A*, 424, 414–424, 1999.
- Bidoli, V., Canestro, A., Casolino, M., et al.: In-orbit performances of the space telescope NINA and GCR fluxes measurements, *Astrophys. J., Supplement Series*, 132, 365–375, 365, 2001.
- Casolino, M., Bidoli, V., de Pascale, M. P., et al.: Launch in orbit of the NINA-2 apparatus aboard the satellite MITA, *Proceeding 27 ICRC (Hamburg)*, 6, 2314–2317, 2001.
- Casolino, M., Bidoli, V., Canestro, A., et al.: Continuation of the mission NINA: NINA-2 experiment on MITA satellite, *Proceeding 26 ICRC (Salt Lake City)*, 5, 136–139, 1999.
- Cook, W. R., Cummings, A. C., Cummings, J. R., et al.: MAST: A Mass Spectrometer Telescope for Studies of the Isotopic Composition of Solar, Anomalous and Galactic Cosmic Ray Nuclei, *IEEE Trans. on Geoscience and Remote Sensing*, 31-3, 557–564, 1993.
- Derome, L., Buenerd, M., Barrau, A., et al.: The origin of the high energy proton component below the geomagnetic cut off detected by the AMS experiment, *Phys. Letts. B*, 489, 1/2, 1–8, 2000.
- GEANT: Detector Description and Simulation Tool, CERN program library, 1994.
- Hasebe, N., Moriya, H., Doke, T., et al.: Improvement of mass resolution of cosmic ray nuclei using a  $\Delta E \times E$  Si detector telescope, *Nucl. Instrum. Methods Phys. Res. A*, 325, 335–342, 1993.
- Lamanna, G., Alpat, B., Battiston, R., et al.: Measurement of deuteron spectra in Low Earth Orbit with the Alpha Magnetic Spectrometer, *Proceeding 27 ICRC (Hamburg)*, 5, 1614–1617, 2001.
- Lipari, P.: The fluxes of sub-cutoff particles detected by AMS, the cosmic ray albedo and atmospheric neutrinos, *Astroparticle physics*, 16, 3, 295–323, 2002.